REMOTE SENSING OF ENVIRONMENT 25:185–199 (1988)

Estimating Big Bluestem Albedo from Directional Reflectance Measurements

J. R. IRONS and K. J. RANSON

NASA/Goddard Space Flight Center, Earth Resources Branch, Greenbelt, Maryland 20771

C. S. T. DAUGHTRY

USDA/ARS Remote Sensing Research Laboratory, Beltsville, Maryland 20705

Total hemispherical shortwave reflectance (albedo) is a major component of the Earth's radiation budget. To develop capabilities for the remote determination of prairie grass albedo, the determination of albedo from spectral bidirectional reflectance data was explored. Estimates of total shortwave albedo were derived from multidirectional reflectance factor measurements of big bluestem (*Andropogon gerardii*) grass acquired during the summer of 1986. The data were analyzed to evaluate the variation of albedo with changes in solar zenith angle and phenology. On any one day, albedo was observed to increase by at least 19% (relative) as solar zenith angle increased. Over the growing season, changes in big bluestem albedo corresponded to changes in the green leaf area index of the grass canopy. The ability to estimate albedo using reflectance factor data acquired within only one or two azimuthal planes and at a restricted range of view zenith angles was also evaluated. Estimates were compared to "true" albedos derived from all available reflectance factor data. Although differences increased slightly with solar zenith angle, estimates derived from data from two azimuthal planes oriented 45° to the solar principal plane were always within 4% (relative) of the "true" albedos even when view zenith angles were restricted to 50° or less. Albedo estimates derived from data along a single azimuthal plane were closest to the "true" albedos when the plane was either the principal or a 45° plane and were always within 10% of the true albedos. Albedo estimates derived from nadir reflectance factor measurements differed by up to 18% from the "true" albedos with the differences increasing with solar zenith angle. Even a limited amount of multiple direction reflectance data proved preferable to a single nadir reflectance factor for the estimation of big bluestem albedo.

Introduction

A comprehensive experiment called the First ISLSCP Field Experiment (FIFE) is being conducted by the National Aeronautics and Space Administration (NASA) with the overall objective of developing methodologies for deriving land surface climatological parameters from satellite radiance measurements (Sellers and Hall, 1987). The approach is to obtain near-surface measurements of parameters determining the radiation budget and surface energy balance and then to compare the near-surface measurements to corresponding values derived from satellite remote sensing data. During 1987, extensive field measurements were made on a 15×15 km site located in the Great Plains (the Konza Prairie near Manhattan, KS) during four 2-week periods from March to October.

As a component of the radiation budget, total hemispherical shortwave reflectance (albedo) is a major parameter of interest to FIFE. Past efforts to estimate albedo from remote sensing data have been constrained by the available instrumentation (Pinker and Ewing, 1986). The available sensors have typically provided directional observations of reflected radiance in narrow spectral bands. Estima-

0034-4257/88/$0.00

tion of albedo from these observations generally required simplifying assumptions. The assumptions included the use of narrow band data to represent reflectance across the short wave portion of the spectrum (0.3–3.0 μm) and an assumption of isotropic (i.e., Lambertian) surface reflectance (Henderson-Sellers and Wilson, 1983; Wiesnet and Matson, 1983). These assumptions are not generally valid for terrestrial reflectance (Coulson, 1966). In particular, relfectance from vegetation varies spectrally and is not isotropic. Several studies have shown that the assumption of isotropic reflectance from vegetation can cause significant inaccuracy in albedo estimates (Eaton and Dirmhirn, 1979; Kimes and Sellers, 1985; Irons et al., 1987). Kimes et al. (1987a) concluded that reflectance observations from multiple view zenith angles along at least a single azimuth direction are required to estimate terrestrial albedos.

Albedos and spectral hemispherical reflectances have been derived from multiple direction observations of bidirectional or biconical reflectance in a number of studies. Kriebel (1979) calculated the total shortwave albedo of four cover types (savannah, bog, pasture land, and coniferous forest) from multiple direction data obtained by an airborne, eight-channel, scanning radiometer. Kimes and Sellers (1985) computed spectral hemispherical reflectances of several bare fields, grass canopies, and row crop canopies from multiple direction observations obtained with a field radiometer. Walthall et al. (1985) developed a three-term equation which describes bidirectional reflectance as a function of view direction relative to the solar direction. The equation was fit to multiple direction data from several bare soil surfaces and a soybean canopy. The equation was then analytically integrated to derive hemispherical reflectances for the various surfaces. Irons et al. (1987) used the equation of Walthall et al. (1985) to estimate the spectral hemispherical reflectances of bare soil, soybeans, and orchardgrass from multiple direction data acquired by a pointable, airborne, imaging radiometer.

New and future sensors offer potential for improving remote estimates of albedo and hemispherical reflectance. Sensors proposed for the future Earth Observing System, for example, will be capable of providing observations over the entire shortwave region from multiple view directions (NASA, 1986). One of the FIFE studies is focusing on the use of multiple view direction data to estimate spectral hemispherical reflectances from the Konza Prairie. The study is using data acquired by an airborne sensor, the Advanced Solid-State Array Spectroradiometer (Barnes et al., 1985), which points through a sequence of fore-to-aft view zenith angles as the airplane flies over a target. The sensor allows view zenith angles out to 45° off-nadir. The FIFE experimental design for the Konza Prairie did limit the multiple direction ASAS observations to one or two azimuthal planes, depending upon the number of flights the airplane was able to make over a particular target.

The work reported here consists of an analysis of reflectance data acquired at multiple view directions with a truck-mounted radiometer over big bluestem (*Andropogon gerardii*) grass during the summer of 1986. Big bluestem is a dominant species in the Konza Prairie (Asrar et al., 1986), and the data are analyzed to evaluate the variation of albedo with changes in solar zenith angle and phenol-

ogy. The ability to estimate albedo using data from only one or two azimuthal planes is also evaluated.

Data

The relationship which describes the bidirectional reflectance of a surface as a function of illuminating geometry (solar zenith and azimuth) and viewing geometry (view zenith and azimuth) is called the bidirectional reflectance distribution function (BRDF). To study the BRDF of plant canopies, bidirectional reflectance factors from multiple view directions were acquired over a number of field plots at Purdue University (Ranson et al., 1985a,b). During the summer of 1986, reflectance measurements were made on a field of big bluestem, a tall perennial warm-season grass. The field had been burned earlier in the year prior to the beginning of spring growth. A Barnes Model 12-1000 Modular Multiband Radiometer (MMR) with 15° field of view was used to measure radiance reflected from the big bluestem in seven spectral bands (Table 1). Spectral reflectance factors were derived from ratios of the spectral radiance reflected from the grass to the spectral radiance reflected from a barium sulfate ($BaSO_4$) painted reference panel (Robinson and Biehl, 1979).

The radiometer was mounted on a boom at 2.3 m above the soil and reflected radiance was measured sequentially at 15 view zenith angles (out to 70° on both sides of nadir in 10° increments) in each of four azimuthal planes for a total of 60 observations. The geometry of these observations is illustrated in Fig. 1. Note that the azimuthal plane of observation is defined by the sensor, the target, and a line through the target perpendicular to the surface. The principal azimuthal plane is defined by the sun, the target, and the perpendicular line through the target.

Big bluestem reflectance factor data were acquired on several dates during the growing season and at several times each day. Table 2 lists the dates and solar zenith and azimuth angles corresponding to each analyzed data set. For each data set, the sequence of 60 directional observations was repeated twice. This pro-

TABLE 1 Downwelling Irradiance at the Earth Surface as a Function of Spectral Band and Solar Zenith Angle.[a]

			Total Downwelling Irradiance in Each Band (W/m^2)					
			Solar Zenith Angle (deg)					
i	Spectral Band (μm)	Corresponding MMR Spectral Band (μm)	17	24	35	47	57	69
1	0.30–0.52	0.45–0.52	147	142	130	110	85	46
2	0.52–0.62	0.52–0.62	120	117	111	100	85	56
3	0.62–0.69	0.63–0.69	72	71	68	63	55	40
4	0.69–1.15	0.75–0.88	286	282	273	255	232	183
5	1.15–1.38	1.15–1.30	66	65	63	60	56	47
6	1.38–1.50		5	5	4	4	3	2
7	1.50–1.85	1.50–1.85	55	54	53	51	49	43
8	1.85–2.08		7	7	6	6	5	4
9	2.08–2.35	2.08–2.35	19	19	19	19	18	16
10	2.35–3.00		4	4	4	3	3	2

[a] Values derived from the LOWTRAN-6 computer code (Kneizys et al., 1983).

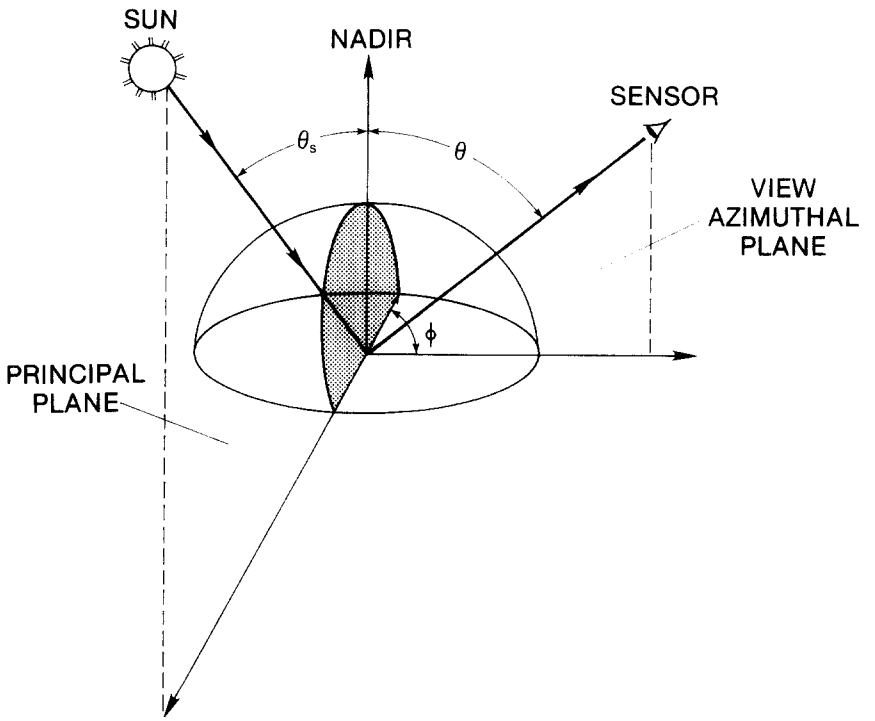

FIGURE 1. Geometry of bidirectional reflectance measurements: θ = view zenith angle; θ_s = solar zenith angle; ϕ = relative azimuth angle.

cess required from 20 to 30 min to complete. Thus, the solar zeniths and azimuths ranged up to 5° on either side of the angles given in Table 2 during data acquisition. In each spectral band, the two reflectance factors for each view direction were averaged, and these average spectral bidirectional reflectance factors were used in the computation of albedo.

Computational Methods

Albedo is the ratio of total shortwave (0.3–3.0 μm) radiation flux reflected by a surface in all directions within the surrounding 2π sr solid angle (i.e., hemisphere) to the total downwelling solar flux. Estimation of big bluestem albedo from the spectral bidirectional reflectance factor data was accomplished by two numerical integrations of the data. The first integration was computed to estimate bidirectional reflectance factors for the shortwave region:

$$\rho = \int_{0.3}^{3.0} \rho(\lambda) E(\lambda)\, d(\lambda) \Big/ \int_{0.3}^{3.0} E(\lambda)\, d(\lambda), \quad (1)$$

$$\rho \simeq \sum_{i=1}^{10} \rho_i E_i \Delta\lambda_i \Big/ \sum_{i=1}^{10} E_i \Delta\lambda_i, \quad (2)$$

where λ indicates wavelength, $\Delta\lambda_i$ represents a spectral band width, E_i represents downwelling spectral irradiance in band i, and ρ_i represents a spectral reflectance factor at a particular view direction in band i.

TABLE 2 Albedos for Big Bluestem Grass during the Growing Season[a]

Date	Solar Azimuth Angle (deg)	Solar Zenith Angle	"True" Albedo	Percent Relative Difference[b]												Nadir Reflectance Factor
				All Available View Zenith Angles in Data Subsets						View Zenith Angles of 50 and Less						
				Azimuthal Planes in Each Data Subset												
				Two[c] Planes	Two[d] Planes	Principal Plane	90° Plane	"Best" 45° Plane	"Worst" 45° Plane	Two[c] Planes	Two[d] Planes	Principal Plane	90° Plane	"Best" 45° Plane	"Worst" 45° Plane	
03 Jun 86	181	18	22.2%	− 1.5%	1.5%	− 3.5%	0.5%	− 0.9%	3.8%	− 2.6%	0.5%	− 4.7%	− 0.5%	− 3.0%	3.9%	− 0.5%
03 Jun 86	99	45	26.3%	− 1.3%	1.3%	3.5%	− 6.0%	− 0.9%	3.3%	− 6.3%	− 1.1%	− 3.0%	− 9.7%	1.2%	− 3.3%	− 17.7%
17 Jun 86	185	17	26.6%	− 0.1%	0.2%	− 2.3%	2.0%	− 1.2%	1.5%	− 0.6%	− 0.6%	− 3.1%	1.8%	0.6%	− 1.9%	− 0.7%
17 Jun 86	231	24	27.4%	− 0.3%	0.2%	− 0.5%	0.0%	− 4.1%	4.5%	− 1.2%	− 0.5%	− 1.5%	− 0.9%	3.8%	− 4.7%	− 6.1%
17 Jun 86	265	47	31.5%	− 0.8%	0.7%	5.8%	− 7.3%	− 0.3%	1.7%	− 4.4%	− 2.1%	1.2%	− 10.0%	− 0.2%	− 4.0%	− 7.2%
17 Jun 86	274	57	34.3%	− 1.4%	1.4%	4.9%	− 7.6%	− 1.0%	3.7%	− 6.0%	− 3.5%	− 0.6%	− 11.5%	0.6%	− 7.7%	− 10.6%
17 Jun 86	283	68	37.5%	− 2.7%	2.7%	9.8%	− 15.3%	− 0.9%	6.5%	− 8.2%	− 2.5%	5.7%	− 22.2%	1.4%	− 6.4%	− 10.7%
03 Jul 86	231	25	28.7%	0.1%	0.0%	2.0%	− 1.9%	2.8%	− 2.9%	− 0.6%	− 0.8%	1.1%	− 2.2%	2.1%	− 3.7%	− 3.3%
03 Jul 86	282	68	37.9%	− 1.3%	1.3%	5.1%	− 7.6%	− 1.9%	4.4%	− 8.9%	− 2.3%	− 3.0%	− 14.7%	1.7%	− 6.4%	− 16.7%
12 Aug 86	135	33	21.6%	− 1.1%	1.1%	0.7%	− 3.0%	− 1.0%	3.2%	− 2.9%	1.1%	− 0.8%	− 5.0%	− 0.8%	3.1%	− 11.9%
Percent RMS difference				1.3%	1.3%	4.6%	6.8%	1.9%	3.8%	5.1%	1.8%	3.0%	10.3%	1.9%	4.8%	10.3%
Reflectance factors per data set			60	30	30	15	15	15	15	22	22	11	11	11	11	1

[a] The "true" albedos were derived from the full sets of available bidirectional reflectance factor data. The relative percent differences are between the "true" albedos and albedo estimates derived from various subsets of the available data.

[b] Percent relative difference = $100*(x-y)/y$, where y is the "true" albedo and x is an albedo estimate derived from a data subset.

[c] Principal plane and the plane perpendicular (90°) to the principal plane.

[d] Two azimuthal planes, each of which are 45° relative to the principal plane.

The short wave region was broken into 10 spectral bands (Table 1) to perform the numerical integration. Reflectance factors in three of the spectral bands (1.38–1.50, 1.85–2.08, and 2.35–3.00 μm) were treated as negligible on the basis of a priori knowledge of typical vegetation reflectance spectra (e.g., Fig. 2). Reflectance factors in the other seven bands were estimated from the measured reflectance factors in the MMR spectral bands (Table 1). Consideration of typical vegetation reflectance spectra (e.g., Fig. 2) indicated that reflectances in the MMR spectral bands were representative of reflectances in the broader spectral bands used for numerical integration.

Downwelling solar flux at the surface is a function of solar zenith, atmospheric conditions, and surface reflectance. The LOWTRAN 6 computer code for atmospheric transmittance (Kneizys et al., 1983) was used to generate solar flux densities in the 10 spectral bands for six solar zenith angles (Table 1). A clear rural atmosphere (23 km visibility) typical of a midlatitude region in the summer was assumed for the flux calculations. In summary, the numerical integration used to derive bidirectional reflectance factors over the short wave region was essentially an average of reflectance factors in 10 spectral bands weighted by the downwelling solar flux in each of the bands. Kriebel (1979) used a similar weighted average of spectral reflectances in his calculations of albedos for several vegetated surfaces. Jackson (1984) has also

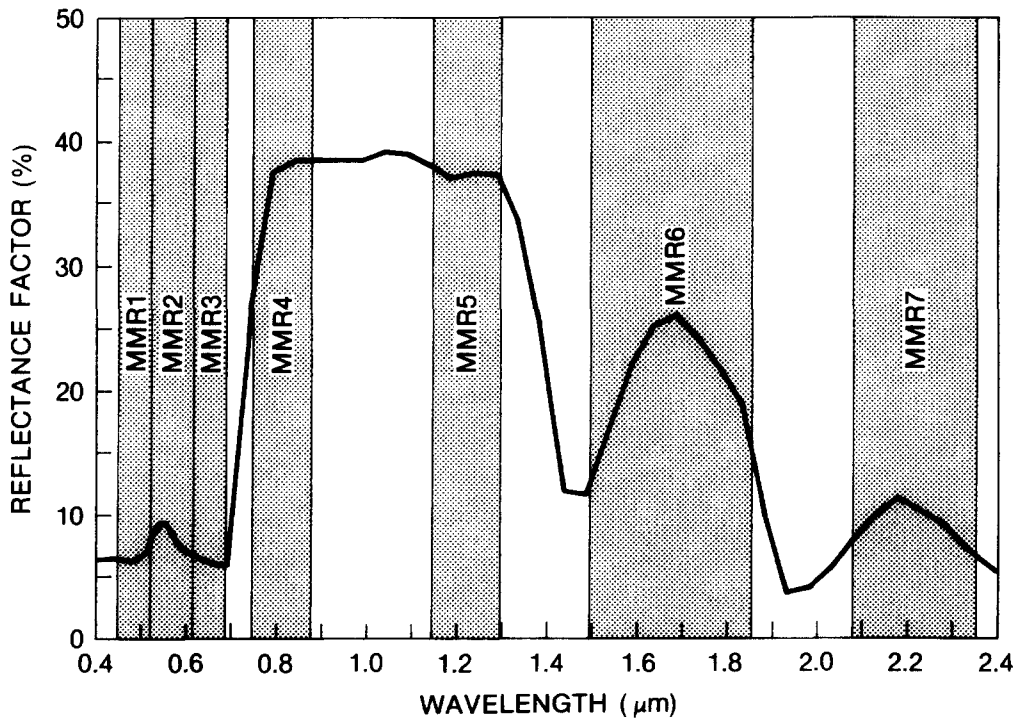

FIGURE 2. Reflectance spectrum of corn leaf provided as an example of typical vegetation reflectance spectra. MMR spectral bands are delineated at the top of the graph.

calculated the total reflected solar radiation from multispectral MMR data using an alternative computational approach.

The second step required to calculate albedos was an integration of bidirectional reflectance factors over the hemisphere surrounding reflecting surfaces. As shown by Kimes and Sellers (1985), albedo is related to a distribution of bidirectional reflectance factors by the following double integral:

$$\alpha = \pi^{-1} \int_{2\pi} \int_{\pi/2} \rho(\theta, \phi) \cos\theta \sin\theta \, d\theta \, d\phi, \tag{3}$$

where α equals albedo, $\rho(\theta, \phi)$ is a distribution of bidirectional reflectance factors at a constant solar zenith angle, θ is the view zenith angle, and ϕ is the relative azimuth angle between the principal plane and the view azimuthal plane. To estimate (3) from the available bidirectional reflectance factors, the following numerical integration was performed:

$$\alpha \simeq \pi^{-1} \sum_{j=1}^{8} \bar{\rho}_j \Delta\Omega_j. \tag{4}$$

To understand (4), consider Fig. 3, which shows the projection of a hemisphere onto a horizontal surface. The hemisphere represents a 2π sr solid angle which contains all the energy reflected by the element of surface area at the center of the hemisphere. The hemisphere has been broken up into eight solid angles which project as annular rings on the horizontal surface. Each jth solid angle is defined by a range of zenith angles and can be envisioned in three dimensions as a hollowed-out cone. Azimuthal planes project as straight lines through the center of the annular rings. The view direction of any bidirectional reflectance measurement can be represented by a point within the annular rings. The angle between a line through the point and the center and the line representing the principal plane defines the relative view azimuth. The distance between the point and the center defines the view zenith angle.

In (4), $\Delta\Omega_j$ equals the projected solid angle represented by each annular ring in Fig. 3:

$$\Delta\Omega_j = \pi\left(\sin^2\theta_j - \sin^2\theta_{j-1}\right). \tag{5}$$

Also in (4), each projected solid angle is multiplied by the average of the bidirectional reflectance factor measurements made within the solid angle (i.e., the average of measurements from view directions represented by points within the appropriate annular ring):

$$\bar{\rho}_j = \sum_{k=1}^{m} \rho\left(\theta_j^*, \phi_k\right)/m, \quad \text{where } \theta_{j-1} < \theta_j^* < \theta_j. \tag{6}$$

The product of $\bar{\rho}_j$ and $\Delta\Omega_j$ is then summed over the eight solid angles (i.e., annular rings) to compute albedo.

The albedos of the observed big bluestem canopy were first derived from (4), (5), and (6) using all of the available bidirectional reflectance factor data. Since measurements were made in four azimuthal planes, a total of eight reflectance values ($m = 8$) were used in (6) for each annular ring except the innermost

ring. An average of four nadir measurements were used for the innermost ring. The albedo estimates derived from the full data sets were treated as "true" albedos in the evaluation of albedo estimates derived from a restricted number of bidirectional reflectance factor measurements.

Estimates of albedo were also derived using data from combinations of two orthogonal azimuthal planes and data from single azimuthal planes. When data were restricted to two planes, the number of reflectance measurements per annular ring was limited to four; i.e., $m = 4$ in (6). One combination of two planes consisted of the principal plane and the plane perpendicular to the principal plane. The other combination consisted of the two planes which form 45° angles with the principal plane. When data were restricted to one plane, two reflectance measurements were averaged per annular ring; i.e., $m = 2$ in (6).

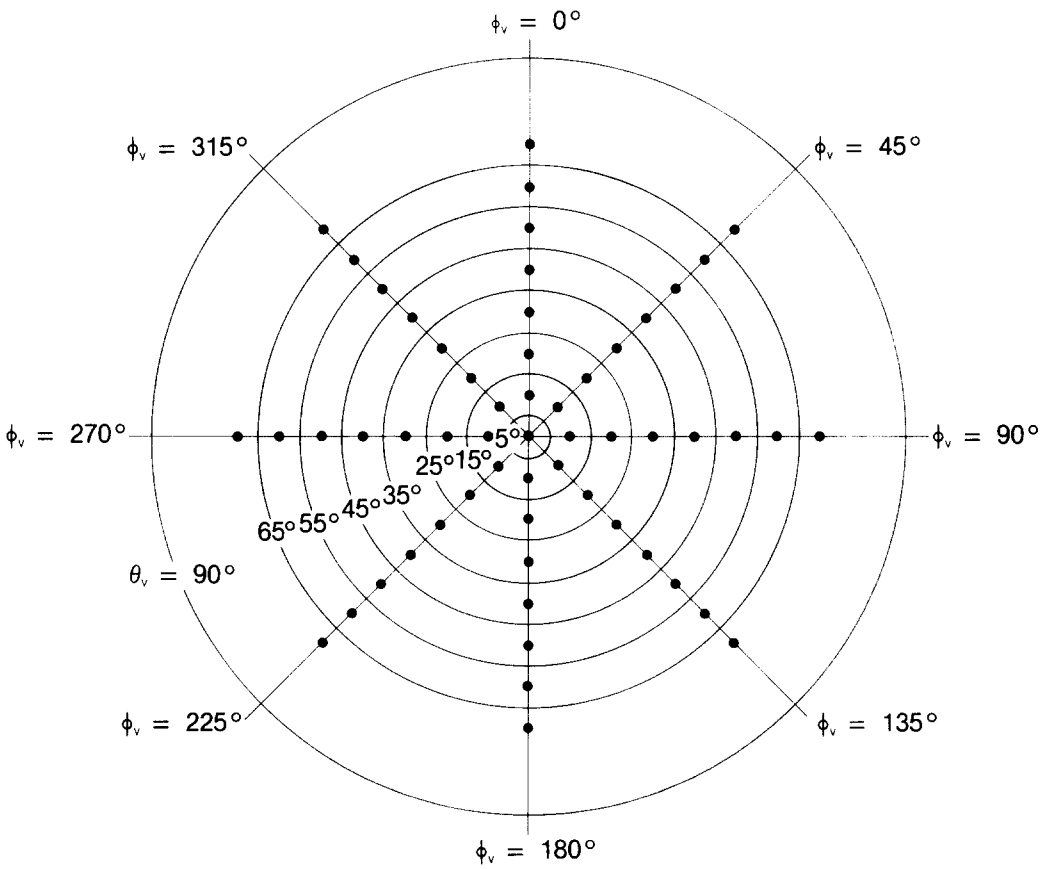

FIGURE 3. Polar plot showing view directions from which bidirectional reflectance factors were measured over the big bluestem field plot. The points locate the view directions. The lines through the center represent the four azimuthal planes on which measurements were taken. The annular rings represent the discrete elements of projected solid angle used in the computation of albedo by numerical integration. ϕ_v = view azimuth angle relative to true north; θ_v = view zenith angle.

For each subset of azimuthal planes, albedo estimation was repeated once with reflectance factor data from all available view zenith angles and once with view zenith angles restricted to 50° or less. When the view zenith angles were restricted, numerical integration was performed using six increments of projected solid angle (i.e., six annular rings). In this case, the outermost ring lay between view zenith angles of 45° and 90°. Albedo estimates derived from the various data subsets were compared to the "true" values derived from the full data sets to evaluate bidirectional reflectance measurement requirements for albedo estimation.

Results and Discussion

The estimates of big bluestem albedo derived from the full data sets are listed in Table 2 and are plotted in Fig. 4 to illustrate trends in albedo. Albedo increased with solar zenith angle on each date. The relative increase ranged from 19 to 41% depending on day and the range of observed solar zenith angles. For nearly equal solar zeniths, albedos increased between June 3 and 17 with only a slight difference in observed albedos between 17 June and 3 July. The one albedo estimate available for 12 August indicated that big bluestem albedo decreased at this stage of the growing season.

Although coincident pyranometer data are not available for direct comparisons, the range and trends of the calculated albedos are consistent with other data in the literature. Increases in the albedo of prairie grass and wheat canopies with increasing solar zenith angle have been noted by several authors (Aase and Idso, 1975; Idso et al., 1978; Kondratyev, 1972; Ripley and Redman, 1976). This trend has also been modeled and discussed by Kimes et al. (1987b). Aase and Idso (1975) used pyranometers to measure diurnal trends of native mixed prairie grass albedo in Montana during the 1973 growing season. The observed albedos ranged from approximately 16 to 30%. Albedos observed in June and July were generally greater than albedos observed in September at comparable solar zenith angles. Kondratyev (1972) provided data showing a diurnal albedo range of approximately 15–30%, with minimums occuring near solar noon, for five grass canopies. Idso et al. (1978) used pyranometers to observe an albedo range of approximately 15–40% over spring wheat plots. Thus the range of calculated big bluestem albedos (22–38%) seems reasonable.

The effect of solar zenith angle on big bluestem albedo can be traced back to the effect of solar zenith angle on big bluestem BRDF. To illustrate, Fig. 5 shows three-dimensional representations of observed reflectance factor distributions at two solar zenith angles. The plane of annular rings in Fig. 3 is represented by the $X-Y$ axes in Fig. 5 with the center of the annular rings located at nadir. Each point within the annular rings defines a view direction, and Fig. 5 contains plots of view direction vs. reflectance factor using a cylindrical coordinate system. Figure 5(a) represents the distribution of big bluestem reflectance factors (total shortwave) observed in 17 June at a solar zenith angle of 17°. Figure 5(b) represents the reflectance factors observed on 17 June at a solar zenith angle of 57°.

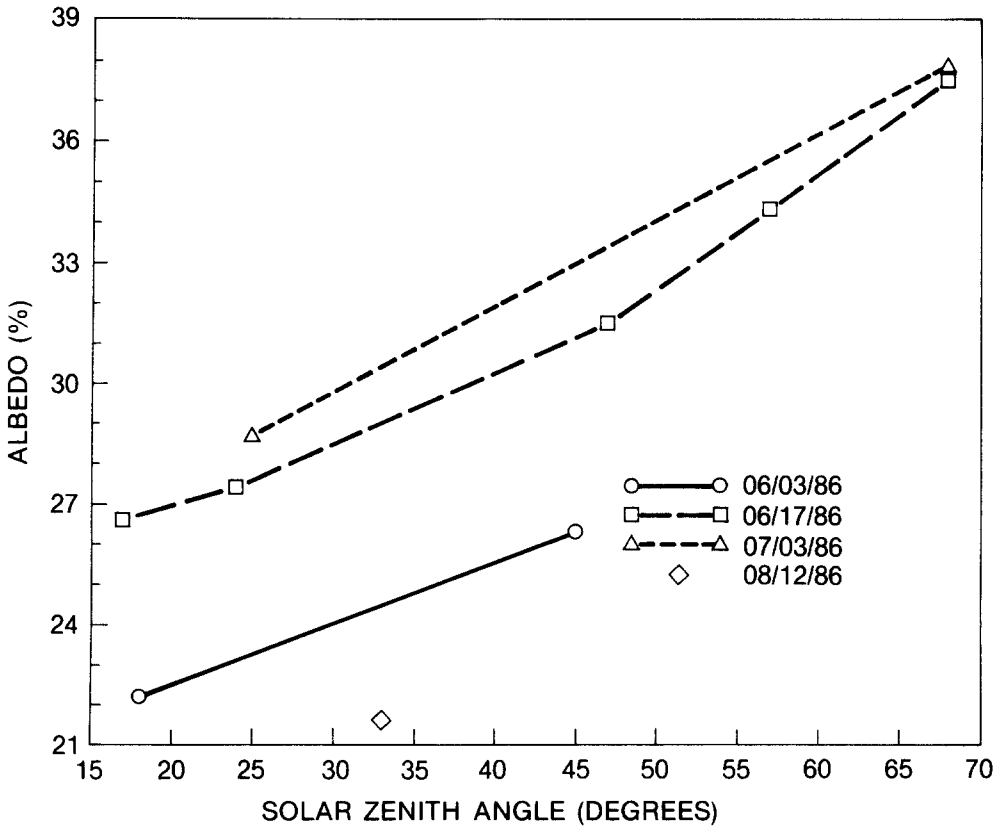

FIGURE 4. Big bluestem albedo versus solar zenith angle for four dates in the 1986 growing season: (○—○) 3 June 1986; (□—□) 17 June 1986; (△—△) 3 July 1986; (◇) 12 August 1986.

At smaller solar zenith angles [Fig. 5(a)], observed reflectance factors showed relatively little variation in reflectance across the view directions. At larger solar zenith angles [Fig. 5(b)], reflectance increased off-nadir. When bidirectional reflectance factors were integrated over all view directions to compute albedo, the increase in off-nadir reflectance at larger solar zeniths resulted in larger albedos relative to the albedos at the smaller solar zenith angles.

The effect of solar zenith angle on plant canopy albedo and reflectance anisotropy can primarily be attributed to a mechanism discussed by Kimes (1983) and Kimes et al. (1987b). Briefly, the mechanism involves the shading of lower canopy layers by the components of the upper canopy as expressed by the probability of gap (i.e., the probability a photon of incident solar radiation can penetrate to any particular canopy layer without first encountering a leaf or other plant component). The probability of gap decreases as the solar zenith angle increases. The probability decrease is greatest in erectophile canopy structures (Kimes et al., 1987b), and the big bluestem canopy structure appears approximately erectophile in photographs of the plants. The result is an increase in the proportion of radiation scattered within the upper canopy layer as solar zenith

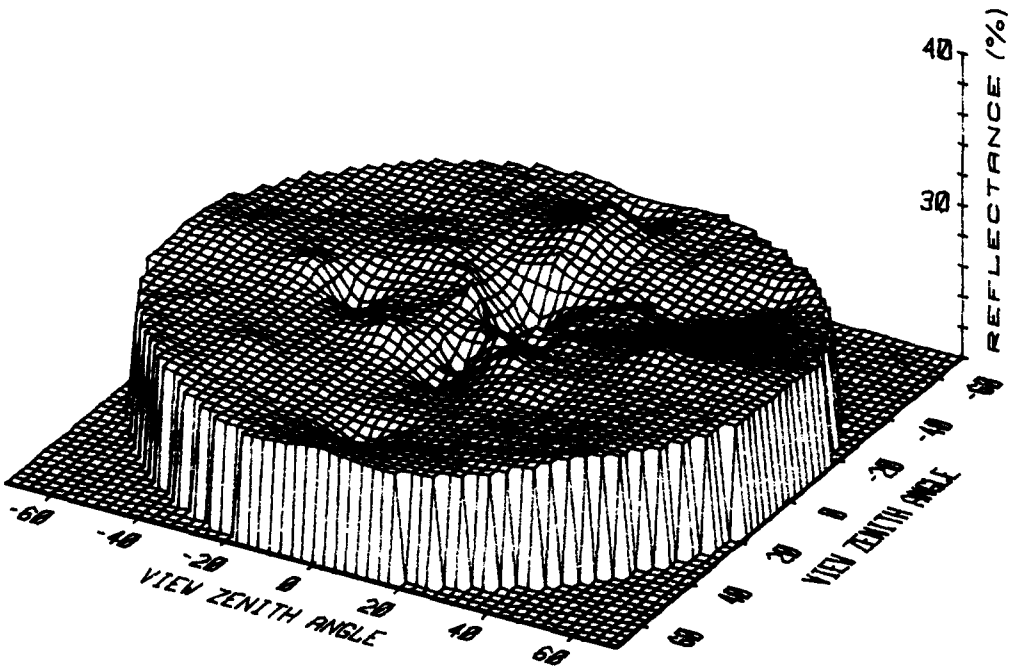

(a)

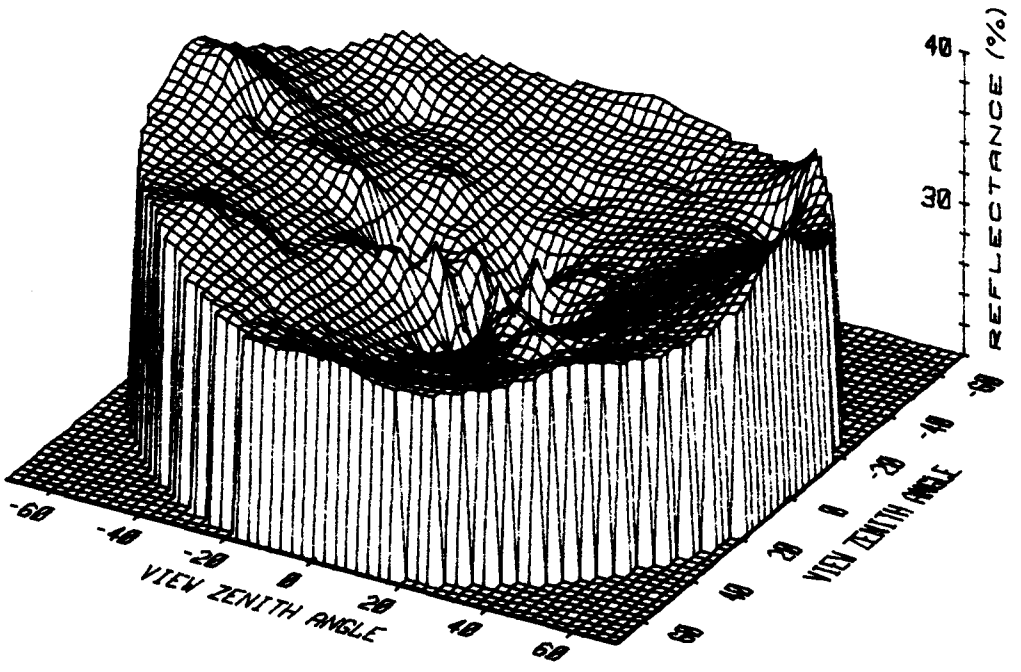

(b)

FIGURE 5. Cylindrical plots of the directional distribution of big bluestem bidirectional reflectance factors (total shortwave) on 17 June, 1986: (a) solar zenith angle of 17°; (b) solar zenith angle of 57°.

angle increases. Photon scattered in the upper layer encounter fewer plant components and are therefore less likely to be absorbed before escaping the canopy. Decreasing the probability of gap also reduces the proportion of photons penetrating to the underlying soil which generally has a lower albedo than the plant components. In addition, the proportion of the lower canopy layers within view is at a maximum from a nadir view direction and decreases as the view zenith angle increases. The overall effect is an increase in off-nadir bidirectional reflectance which becomes more pronounced as the solar zenith angle increases.

The changes in big bluestem albedo over the summer are related to the changes in the grass canopy structure and composition as the plants developed. Table 3 provides data on canopy phytomass and leaf area acquired over the growing season. Albedo appears to correspond most closely to green leaf area index (LAI). That is, the dates of generally lowest (12 August) and highest (3 July) observed albedo coincided with the dates of lowest and highest green LAI. Both the green LAI and albedo were observed to increase through the tillering and jointing growth stages of early summer. Although the observed albedo was lowest on 12 August, the big bluestem had reached the heading stage and had begun to become senescent resulting in less green leaf area to absorb photosynthetically active radiation (0.4–0.7 μm). The lower albedo was likely due to decreased near infrared reflectance by the plant canopy at this stage of development (Asrar et al., 1986).

Table 2 also lists the percent relative difference between "true" albedos derived from the full reflectance factor data sets and the albedo estimates derived from subsets of the data. When data from the full range of view zenith angles were used, albedo estimates derived from data from two orthogonal azimuthal planes corresponded closely to the "true" estimates. The differences increased slightly with solar zenith angle but never exceeded 3%. The estimates from the two 45° azimuthal planes were always slightly larger than the "true" values whereas the estimates derived from combining data from the principal plane and the perpendicular plane (90°) were always slightly less than the "true" values.

When the reflectance factor data were restricted to view zenith angles of 50° or less, the estimates derived from the two 45° azimuthal planes still closely approximated the "true" albedos. These

TABLE 3 Phytomass and Leaf Area of Big Bluestem Grass Canopy during the 1986 Growing Season.[a]

Date	Total Fresh Phytomass (g/m^2)	Dry Phytomass (g/m^2)					
		Total	Green Leaves	Brown Leaves	Stems[b]	Height (m)	Green LAI
04 Jun 86	1302	253	148	0	104	0.2	3.1
19 Jun 86	1837	394	247	14	133	0.6	4.9
07 Jul 86	2248	653	381	72	200	1.2	5.8
14 Aug 86	2207	854	237	243	375	1.5	2.3

[a] Values are means of five 0.1 m^2 samples.
[b] Stems include culms, leaf sheaths, and inflorescence, when present.

estimates usually underestimated the "true" values and the error generally increased with increasing solar zenith angle, but the relative differences were always less than 4%. The albedo estimates derived from restricted view zenith angles along the principal and 90° planes varied by as much as 9% from the "true" albedos. Again, the error increased as the solar zenith angle increased.

If big bluestem BRDF was symmetric about the principal plane, albedo estimates derived from data acquired along one 45° azimuthal plane should have equaled the estimate derived from the other 45° plane. The results shown in Table 2 indicate that this was not the case. The lack of agreement of derived albedos between the two 45° planes could have been due to asymmetry of the BRDF or experimental uncertainty in the original reflectance factor measurements, or both. The estimates derived from combining data acquired along both 45° azimuthal planes were generally closer to the "true" albedo than estimates derived from either single azimuthal plane even when the view zenith angle range was restricted.

The albedo estimates derived from data along a single azimuthal plane were closest to the "true" albedos when the plane was either the principal plane or a 45° plane. When all view zenith angles were considered, the root mean square (RMS) difference was slightly greater for estimates derived from the principal plane data (4.63%) than the RMS difference from the worst of the two estimates derived from the data along a 45° plane (3.81%). When view zenith angles were restricted, the RMS difference for principal plane data (1.79%) was slightly less than the RMS difference for the best of the two estimates derived from data along a 45° azimuthal plane (1.89%). In comparison, Kimes et al. (1987a) found data from the 45° azimuthal plane preferable for the estimation of terrestrial albedos when data were available from view zenith angles on both sides of nadir from a single azimuthal plane.

Nadir bidirectional reflectance factors only provided close approximations to "true" albedo at small solar zenith angles. At solar zenith angles greater than 25°, the nadir reflectance factor underestimated "true" albedo by 7–18%. This result is again traceable to the previously discussed effect of solar zenith angle on the anisotropy of big bluestem reflectance. At the small solar zenith angles, the reflectance varies less with view direction, and a single bidirectional reflectance factor observation from any view direction would approximate the albedo. As solar zenith angle increases, the anisotropy of reflectance also increases with larger reflectance factors occurring off-nadir. The reflectance factors observed from nadir thus underestimate the albedo at large solar zenith angles.

These results have implications for the design of experiments such as FIFE. Two flights over a site in orthogonal directions appear adequate for the remote determination of prairie grass albedo using a pointable sensor such as ASAS. Given the maximum ASAS view zenith angle of 45°, the preferable flight directions are along lines 45° from the solar principal plane. If only one flight line is possible, then it should be chosen either along the principal plane or 45° from the principal plane. Regardless of the flight line orientation, estimates of albedo derived from multiple view direction ASAS or other pointable sensor should prove more accu-

rate than albedo estimates from single nadir reflectance factors, particularly for albedos at large solar zenith angles.

This study was supported in part by NASA Headquarters, Land Processes Branch and Goddard Space Flight Center, Earth Resources Branch. The authors would like to thank D. Locks, J. Roecker, and M. Resch of Purdue University for assistance with the field measurements.

References

Aase, J. K., and Idso, S. B. (1975), Solar radiation interactions with mixed prairie rangeland in natural and denuded conditions, *Arch. Met. Geophys. Biokl. Ser. B* 23:255–264.

Asrar, G., Weiser, R. L., Johnson, D. E., Kanemasu, E. T., and Killeen, J. M. (1986), Distinguishing among the tallgrass prairie cover types from measurements of multispectral reflectance, *Remote Sens. Environ.* 19(2):159–169.

Barnes, W. L., Huegel, F. G., and Irons, J. R. (1985), An airborne imaging system for measuring anisotropic reflectance patterns, in *Proceedings, Pecora* 10, Remote Sensing in Forest and Range Resource Management, Fort Collins, CO, pp. 508–516.

Coulson, K. L. (1966), Effects of reflection properties of natural surfaces in aerial reconnaissance, *Appl. Opt.* 5(6):905–917.

Eaton, F. D., and Dirmhirn, I. (1979), Reflectance irradiation indicatrices of natural surfaces and their effect on albedo, *Appl. Opt.* 18(7):994–1008.

Henderson-Sellers, A., and Wilson, M. F. (1983), Surface albedo data for climatic modeling, *Rev. Geophys. Space Phy.* 21(8):1743–1778.

Idso, S. B., Hatfield, J. L., Reginato, R. J., and Jackson, R. D. (1978), Wheat yield estimation by albedo measurement, *Remote Sens. Environ.* 7:273–276.

Irons, J. R., Johnson, B. L., Jr., and Linebaugh, G. H. (1987), Multiple-angle observations of reflectance anisotropy from an airborne linear array sensor, *IEEE Trans. Geosci. Remote Sens.* GE-25(3):372–383.

Jackson, R. D. (1984), Total reflected solar radiation calculated from multi-band sensor data, *Agric. Forest Meteorol.* 33:163–175.

Kimes, D. S. (1983), Dynamics of directional reflectance factor distributions for vegetation canopies, *Appl. Opt.* 22:1364–1372.

Kimes, D. S., and Sellers, P. J. (1985), Inferring hemispherical reflectance of the earth's surface for global energy budgets from remotely sensed nadir of directional radiance values, *Remote Sens. Environ.* 18:205–223.

Kimes, D. S., Sellers, P. J., and Diner, D. J. (1987a), Extraction of spectral hemispherical reflectance (albedo) of surfaces from nadir directional reflectance data, *Int. J. Remote Sens.* 8(12):1727–1746.

Kimes, D. S., Sellers, P. J., and Newcomb, W. W. (1987b), Hemispherical reflectance variations of vegetation canopies and implications for global and regional energy budget studies, *J. Climate Appl. Meteorol.* 26(8):959–972.

Kneizys, F. X., Shettle, E. P., Gallery, W. O., Chetwynd, J. H., Jr., Abeau, L. W., Selby, J. E. A., Clough, S. A., and Fenn, R. W. (1983), Atmospheric transmittance/radiance: computer code LOWTRAN 6. Environmental Research Papers No. 846, Optical Physics Division, Air Force Geophysics Laboratory, Hanscom AFB, MA.

Kondratyev, K. Ya. (1972), *Radiation Processes in the Atmosphere*, WMO-No. 309, World Meteorological Organization.

Kriebel, K. T. (1979), Albedo of vegetated surfaces: its variability with differing irradiances, *Remote Sens. Environ.* 8:283–290.

NASA (1986), MODIS: moderate-resolution imaging spectrometer instrument panel report, in *Earth Observing Reports, Vol. IIb*, NASA/Headquarters, Code NIT-4, Washington, DC 20546, 59 pp.

Pinker, R. T., and Ewing, J. A. (1986), Effect of surface properties on the narrow to broadband spectral relationship in clear sky satellite observations, *Remote Sens. Environ.* 20:267–282.

Ranson, K. J., Biehl, L. L., and Bauer, M. E. (1985a), Variation in spectral response of soybeans with respect to illumination, view and canopy geometry, *Int. J. Remote Sens.* 6(12):1827–1842.

Ranson, K. J., Daughtry, C. S. T., Biehl, L. L., and Bauer, M. E. (1985b), Sun-view angle effects on reflectance factors of corn canopies, *Remote Sens. Environ.* 18:147–161.

Ripley, E. A., and Redman, R. E. (1976), Grassland, in *Vegetation and the Atmosphere, Vol.* 2 (J. L. Monteith, Ed.), Academic, London.

Robinson, B. F., and Biehl, L. L. (1979), Calibration procedures for measurement of reflectance factor in remote sensing field research, in *Proceedings of the Society of Photo-Optical Instrumentation Engineering*, 23rd Annual Technical Symposium on Measurements of Optical Radiation, Bellingham, WA, pp. 16–26.

Sellers, P. J., and Hall, F. G., Eds. (1987), The FIFE experiment plan, NASA/GSFC Earth Resources Branch, Greenbelt, MD 20771.

Walthall, C. L., Norman, J. M., Welles, J. M., Campbell, G., and Blad, B. L. (1985), Simple equation to approximate the bidirectional reflectance from vegetative canopies and bare soil surfaces, *Appl. Opt.* 24(3):383–387.

Wiesnet, D. R., and Matson, M. (1983), Remote sensing of weather and climate, in *Manual of Remote Sensing* 2nd ed., Vol. II (J. E. Estes and G. A. Thorley, Eds.), American Society of Photogrammetry, Falls Church, VA.

Received 12 August 1987; revised 9 February 1988.